

Journal of Geophysical Research: Solid Earth**RESEARCH ARTICLE**

10.1002/2015JB012616

Key Points:

- Slow mantle velocities delineate a thermal anomaly beneath Marie Byrd Land, possibly representing a mantle plume
- Seventy kilometer thick high-velocity lithosphere beneath the West Antarctic Rift System limits average heat flow to less than 90 mW/m^2
- Ellsworth-Whitmore mantle lithosphere has intermediate velocity suggesting a Precambrian block with tectonic alteration

Supporting Information:

- Table S1

Correspondence to:

D. A. Wiens,
doug@wustl.edu

Citation:

Heeszel, D. S., D. A. Wiens, S. Anandakrishnan, R. C. Aster, I. W. D. Dalziel, A. D. Huerta, A. A. Nyblade, T. J. Wilson, and J. P. Winberry (2016), Upper mantle structure of central and West Antarctica from array analysis of Rayleigh wave phase velocities, *J. Geophys. Res. Solid Earth*, 121, 1758–1775, doi:10.1002/2015JB012616.

Received 21 OCT 2015

Accepted 29 JAN 2016

Accepted article online 4 FEB 2016

Published online 7 MAR 2016

Upper mantle structure of central and West Antarctica from array analysis of Rayleigh wave phase velocities

David S. Heeszel^{1,2}, Douglas A. Wiens¹, Sridhar Anandakrishnan³, Richard C. Aster⁴, Ian W. D. Dalziel⁵, Audrey D. Huerta⁶, Andrew A. Nyblade³, Terry J. Wilson⁷, and J. Paul Winberry⁶

¹Department of Earth and Planetary Sciences, Washington University, St. Louis, Missouri, USA, ²United States Nuclear Regulatory Commission, Washington, District of Columbia, USA, ³Department of Geosciences, Pennsylvania State University, University Park, Pennsylvania, USA, ⁴Geosciences Department, Warner College of Natural Resources, Colorado State University, Fort Collins, Colorado, USA, ⁵Institute for Geophysics, University of Texas at Austin, Austin, Texas, USA, ⁶Department of Geological Sciences, Central Washington University, Ellensburg, Washington, USA, ⁷Department of Geological Sciences, Ohio State University, Columbus, Ohio, USA

Abstract The seismic velocity structure of Antarctica is important, both as a constraint on the tectonic history of the continent and for understanding solid Earth interactions with the ice sheet. We use Rayleigh wave array analysis methods applied to teleseismic data from recent temporary broadband seismograph deployments to image the upper mantle structure of central and West Antarctica. Phase velocity maps are determined using a two-plane wave tomography method and are inverted for shear velocity using a Monte Carlo approach to estimate three-dimensional velocity structure. Results illuminate the structural dichotomy between the East Antarctic Craton and West Antarctica, with West Antarctica showing thinner crust and slower upper mantle velocity. West Antarctica is characterized by a 70–100 km thick lithosphere, underlain by a low-velocity zone to depths of at least 200 km. The slowest anomalies are beneath Ross Island and the Marie Byrd Land dome and are interpreted as upper mantle thermal anomalies possibly due to mantle plumes. The central Transantarctic Mountains are marked by an uppermost mantle slow-velocity anomaly, suggesting that the topography is thermally supported. The presence of thin, higher-velocity lithosphere to depths of about 70 km beneath the West Antarctic Rift System limits estimates of the regionally averaged heat flow to less than 90 mW/m^2 . The Ellsworth-Whitmore block is underlain by mantle with velocities that are intermediate between those of the West Antarctic Rift System and the East Antarctic Craton. We interpret this province as Precambrian continental lithosphere that has been altered by Phanerozoic tectonic and magmatic activity.

1. Introduction

The upper mantle seismic structure of Antarctica provides insight into the geological and tectonic history of the continent, which is poorly understood due to very limited geological exposure as a result of the thick ice sheet. Seismic structure can also provide important constraints on factors that control interactions between the solid Earth and the ice sheet, including the estimates of lithospheric strength and mantle viscosity structure required for glacial isostatic adjustment modeling [Wiens and Sammis, 1995; van der Wal et al., 2015] and for heat flow at the base of the ice sheet [Shapiro and Ritzwoller, 2004; Pollard et al., 2005; Larour et al., 2012].

Due to the challenges associated with deploying seismometers in the harsh climate of Antarctica, the seismic velocity structure of the continent to date has primarily been estimated through continent-scale studies based on teleseismic surface waves recorded at sparse permanent seismic stations [Roult and Rouland, 1992; Danesi and Morelli, 2000, 2001; Ritzwoller et al., 2001; Morelli and Danesi, 2004]. The earliest regional tomography studies using temporary seismic networks and methods that are commonly used on other continents occurred in the TAMSEIS project [Lawrence et al., 2006a, 2006b, 2006c; Watson et al., 2006; Pyle et al., 2010] which provided insight into the structure and tectonic setting of the Transantarctic Mountains (TAM) in the South Victoria Land and Ross Sea region.

Recent large-scale deployments of temporary broadband seismic stations in West Antarctica (POLENET/ANET) and in central East Antarctica (AGAP/GAMSEIS) now make it possible to seismically image much of the Antarctic continent at a new level of resolution. Recent studies have used these data to derive large-scale body wave [Hansen et al., 2014] and surface wave [An et al., 2015] models of the Antarctic region, and to

constrain crustal thicknesses [Chaput *et al.*, 2014] and seismic anisotropy [Accardo *et al.*, 2014]. In this paper, we utilize a comprehensive data set from these recent deployments, in conjunction with array-based phase velocity determination techniques, to obtain new surface wave models of the upper mantle beneath Antarctica. The data set used combines POLENET/ANET, AGAP/GAMSEIS, TAMSEIS, and other data from the sparse network of permanent Antarctic seismic stations to perform teleseismic Rayleigh wave phase velocity tomography using the two-plane wave method of Forsyth and Li [2005]. We then invert the derived phase velocity maps for a three-dimensional shear velocity structural model and discuss the implications of the velocity variations for the structure and tectonic history of Antarctica.

2. Tectonic Setting

The large-scale tectonic framework of Antarctic continental interior is subject to many uncertainties. With the exception of rock outcrops near the edges of the continent and in the TAMS, which define the boundary between East and West Antarctica, direct sampling of bedrock is limited due to the thick ice cover. Therefore, knowledge of the geologic structure and tectonic history is based almost solely on extrapolating observations from the limited surface geological exposures, guided by the interpretation of subglacial topography in association with aerogeophysical, seismic, gravity, and magnetic data. In this section, we briefly outline the tectonic setting and history of the study region.

The Gamburtsev Subglacial Mountains (GSM) in East Antarctica are poorly understood, in large part due to a complete absence of geological samples, and their history and tectonic origin is widely debated [van de Flierdt *et al.*, 2008; Hansen *et al.*, 2010; Ferraccioli *et al.*, 2011]. Various tectonic scenarios have been presented to link geological evidence from the periphery with possible tectonic effects on the interior [Fitzsimons, 2000a, 2000b, 2003; Goodge and Fanning, 2010; Boger, 2011]. The AGAP/GAMSEIS investigation revealed highly thickened crust [Hansen *et al.*, 2010] and fast lithosphere extending to depths of about 250 km [Heeszel *et al.*, 2013; Lloyd *et al.*, 2013]. These studies hypothesized that the modern GSM are of Permian age and represent a reactivation of an older structure, with the age of the continental lithosphere in the region dating to the Archean and Paleoproterozoic. A series of subglacial basins and intervening highlands lie between the GSM and the TAMS. The basins represent major subglacial topographic lows, and their large-scale, internal structure is known primarily through geophysical studies [Stern and ten Brink, 1989; ten Brink and Stern, 1992; ten Brink *et al.*, 1993; Studinger *et al.*, 2004; Ferraccioli *et al.*, 2009; Pyle *et al.*, 2010].

The TAMS are a 2500 km long noncompressional mountain range that marks the tectonic boundary between East and West Antarctica and originated in the Neoproterozoic when another craton, possibly Laurentia, drifted away [Dalziel, 1991]. Through geologic time, the region has undergone multiple instances of orogenesis including the Nimrod (~1.7 Ga) [Goodge *et al.*, 2001] and the Ross-Delamaran orogenies (550–450 Ma) [Fitzsimons, 2000a]. Late Mesozoic to Cenozoic uplift of the TAMS has been suggested to result from flexural uplift associated with the growth of the West Antarctic Rift System (WARS) [Stern and ten Brink, 1989; ten Brink and Stern, 1992; ten Brink *et al.*, 1993], crustal thickening [Studinger *et al.*, 2004], or a hybrid model of these two effects [Lawrence *et al.*, 2006a].

West Antarctica is composed of several crustal blocks that have undergone motion relative to each other and the East Antarctic craton [Dalziel and Elliot, 1982; Jankowski and Drewry, 1981]. The WARS, extending from the Ross Sea to the Ellsworth-Whitmore and Antarctic Peninsula blocks, has undergone continental rifting beginning in the Mesozoic and extending into the Cenozoic [Cooper and Davey, 1985; Davey and Brancolini, 1995; Wilson, 1995; Siddoway, 2008]. Deep topographic lows and basin-scale features mapped by aerogeophysical techniques have been interpreted as representing rift basins [Jordan *et al.*, 2010], and locally thinned continental crust is associated with the most prominent of these [Winberry and Anandakrishnan, 2004; Chaput *et al.*, 2014]. Evidence from the Ross Sea Embayment indicates that multiple extension pulses are required to fit paleomagnetic constraints [DiVenere *et al.*, 1994; Cande *et al.*, 2000; Davey *et al.*, 2006; Wilson and Luyendyk, 2006]. This evidence indicates large-scale extension of the WARS ending at about 48 Ma, followed by possible transcurrent or transpressional motion between 48 and 17 Ma [Wilson and Luyendyk, 2009; Granot *et al.*, 2010, 2013]. A final phase of extension is inferred beginning at 17 Ma, coincident with highly localized extension and crustal thinning at the Terror Rift bordering the TAMS in the Ross Sea Embayment [Henrys *et al.*, 2007; Fielding *et al.*, 2008; Granot *et al.*, 2010]. This is consistent with geodynamic modeling that

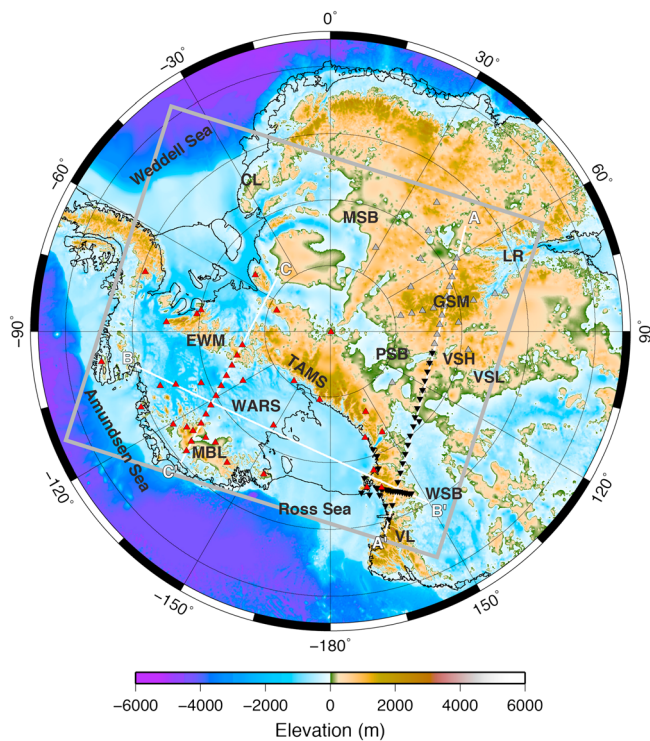


Figure 1. Seismic station locations and geographical regions on a map of subglacial bedrock topography [Fretwell et al., 2013]. Heavy grey line outlines the study region. Station locations are grey (GAMSEIS), black inverted (TAMSEIS), or red (POLENET/ANET) triangles depending on seismic network. Major subglacial features are labeled in red: LR, GSM, VSH, VSL, MSB, PSB, WSB, TAMS, EWM, WARS, MBL, CL, and VL are the Lambert Rift, Gamburtsev Subglacial Mountains, Vostok Subglacial Highlands, Vostok Subglacial Lake, Maud Subglacial Basin, Polar Subglacial Basin, Wilkes Subglacial Basin, Transantarctic Mountains, Ellsworth Whitmore Mountains, West Antarctic Rift System, Marie Byrd Land, Coates Land, and Victoria Land, respectively. A-A', B-B', and C-C' denote locations of cross sections in Figure 8.

for the thermal influence of a deep seated plume, thinning is found in adjacent regions [Emry et al., 2015], perhaps indicating a deflected plume. An inferred ~3 km of uplift since 28–30 Ma also supports a plume hypothesis for the development of the Marie Byrd Land dome [LeMasurier and Landis, 1996].

3. Data and Methods

3.1. Seismic Arrays and Data Selection

Data for this study were collected from three large temporary broadband seismic deployments (TAMSEIS, AGAP/GAMSEIS, and POLENET/ANET) and by three permanent seismic stations. This station distribution enables us to image the structure from the GSM throughout most of West Antarctica (Figure 1). The TAMSEIS array (Lawrence et al., 2006a) was a temporary network of 42 seismic stations that collected data during the austral summers of 2001–2003. The deployment consisted of three components: a coastal array on the Ross Sea in the region of Ross Island; an east-west array extending from McMurdo station, across the TAMS and onto the East Antarctic Ice Sheet; and a long, crossing array that ran from Terra Nova Bay, over the TAMS, and onto the East Antarctic Ice Sheet. The AGAP/GAMSEIS network was a multinational deployment of 28 broadband seismic stations designed to study the seismic structure of the GSM as an element of the 2007–2009 International Polar Year [Hansen et al., 2010; Heeszel et al., 2013]. The network consisted of two lines of stations that crossed near dome A, one an extension of the long TAMSEIS line and the other a north-south line.

supports a progression from a broad region of extension during the early stages of WARS formation to a more focused form of extension near the TAMS during later stages [Huerta and Harry, 2007].

The WARS is bounded to the southeast by the Ellsworth-Whitmore block, a fragment of the margin of the East Antarctic craton that has separated, translated, and rotated into West Antarctica [Schopf, 1969; Dalziel and Elliot, 1982; Grunow et al., 1991; Randall and Mac Niocaill, 2004]. Marie Byrd Land, defining the complementary edge of the rift system, is an uplifted region that has undergone Paleozoic through Cenozoic magmatic activity [Hole and LeMasurier, 1994; Panter et al., 1997; Corr and Vaughan, 2008; Paulson and Wilson, 2010; Lough et al., 2013] and shows somewhat thicker crust [Chaput et al., 2014]. Recent work supports a plume hypothesis for uplift of Marie Byrd Land. Lines of evidence include igneous rocks with a geochemical plume affinity [Weaver et al., 1994; Panter et al., 1997] and deep seated low-velocity anomalies observed seismically [Sieminski et al., 2003; Hansen et al., 2014]. Although there is no prominent thinning of the transition zone immediately beneath the volcanism as might be expected

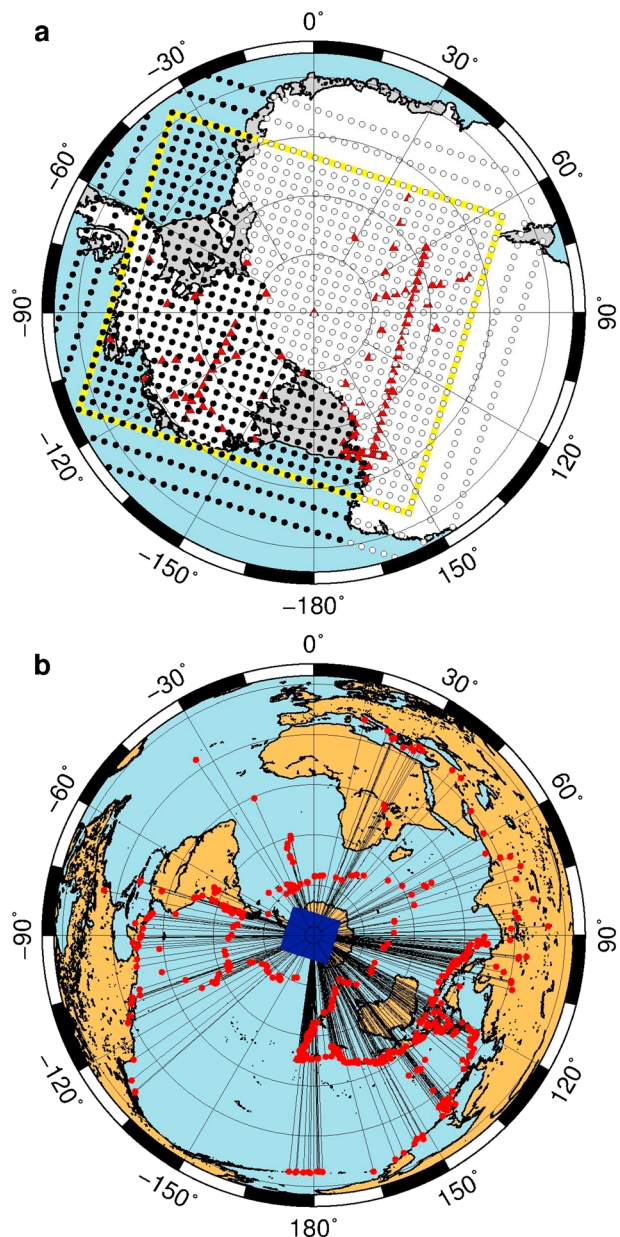


Figure 2. Map of (a) model nodes and (b) earthquakes used in this study. Nodes in black are associated with West Antarctica, and those in white are associated with East Antarctica in the regionalization and in Figure 3 (Figure 2a). Red triangles are seismic stations, and the imaged region is outlined in yellow. Earthquakes used in this study are shown in red with lines showing the approximate propagation path to the array (Figure 2b). Events show a good azimuthal distribution relative to the study area. The blue rectangle denotes the imaged region and corresponds to yellow outline in Figure 2a.

at 25 period bands between 18 and 182 s and then apply a time window around the fundamental mode Rayleigh waves.

3.2. Phase Velocity Inversion

We determine the Rayleigh wave phase velocity as a function of period and position using the two-plane wave method [Forsyth and Li, 2005]. This method utilizes both phase and amplitude information to model the incoming surface wave as the interference of two plane waves. The method improves on traditional

The third temporary network utilized in this study is the POLENET/ANET deployment across West Antarctica [Accardo et al., 2014; Chaput et al., 2014], from which we analyze data recorded by 39 stations during 2008–2012. This network was designed to study the crustal and upper mantle structure of West Antarctica. Two elements of POLENET/ANET are utilized here; a longer-term backbone array and a linear transect of temporary stations deployed from early 2010 to early 2012 extending from the Whitmore Mountains across the West Antarctic Rift System (WARS) to Marie Byrd Land. Our imaging also utilized data from three permanent stations associated with the Global Seismographic Network: QSPA at South Pole, VNDA in the McMurdo Dry Valleys, and SBA on Ross Island. We parameterize the imaged sector of Antarctica using a grid of nodes (Figure 2a). Our methods require a spacing of no greater than a few hundred kilometers between seismic stations, so we do not solve for the velocity in regions with extremely sparse station distribution (masked regions in Figures 4–7).

We select global earthquakes shallower than 100 km based on distance from the array and the surface wave magnitude of the earthquake (Figure 2b). For epicentral distances between 30° and 60° we examine earthquakes with $M_S \geq 4.5$, whereas for distances of 60°–150° we apply a larger magnitude threshold of $M_S \geq 5.5$. We applied a less stringent magnitude requirements for earthquakes occurring nearer the study region to allow the use of more earthquakes located along the circum-Antarctic ridge system and in the subduction zones of the Southern Hemisphere. Instrument response is removed from all data, and we visually inspect data to eliminate records with low signal-to-noise ratio or data dropouts and other artifacts. We filter high-quality data with a two-pass four-pole Butterworth filter

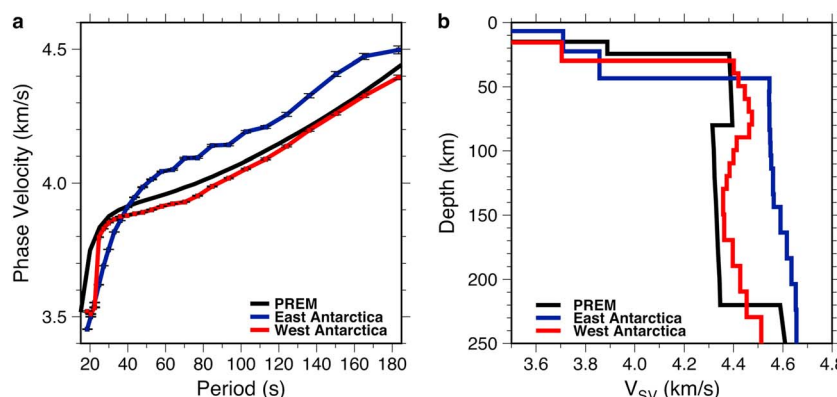


Figure 3. (a) Average 1-D phase velocity and (b) vertically polarized shear velocity for East Antarctica (blue) and West Antarctica (red) compared to the Preliminary Reference Earth Model (PREM) S_V global model (black) [Dziewonski and Anderson, 1981]. East Antarctica is characterized by a much thicker crust and much faster mantle compared to PREM, which is dominated by oceanic structure. In contrast, West Antarctica shows a dispersion curve and velocity structure much more similar to PREM. Note that the PREM model is referenced to 200 s period, whereas the models in this study are not referenced to a particular period due to the lack of a reliable attenuation model.

two-station surface wave tomography methods by better accommodating effects due to wavefield scattering, multipathing, and off-great circle path effects [Li *et al.*, 2003; Forsyth and Li, 2005]. We further utilize modifications to the method that reduce the effect of off-great circle path energy by including 2-D sensitivity kernels in the inversion [Yang and Forsyth, 2006] that are based on the Born approximation [Zhou *et al.*, 2004]. The processing and inversion methods used here are very similar to those applied in a smaller-scale study around the Gamburtsev Subglacial Mountains [Heeszel *et al.*, 2013].

The two-plane wave method may encounter problems with continent-scale arrays, in that the imaging region is too large for the wavefronts to be adequately approximated as plane waves. To preserve the usefulness of the plane wave assumption, we adopt an approach in which we divide the large seismic array into multiple smaller subarrays (Table S1 in the supporting information) and process a single earthquake observed across the entire array as a separate event within each subarray following the method of Yang *et al.* [2008]. This allows us to preserve the plane wave assumption locally and to jointly invert all of the data simultaneously to produce a single phase velocity model [Yang *et al.*, 2008]. An alternative to this approach is to invert for each subarray separately and average regions of overlap [Yang and Ritzwoller, 2008]. However, this approach adds computational complexity and could create subarray boundary artifacts.

In the first stage of the inversion process, we solve for the average phase velocity as a function of period across the East Antarctic and West Antarctic subregions (Figure 2a). This division is necessary because the crust and upper mantle velocity structure in the two regions differ greatly [Danesi and Morelli, 2001; Ritzwoller *et al.*, 2001; Lawrence *et al.*, 2006a; Block *et al.*, 2009], and it is necessary to have a reasonable starting model in each region for the inversion to converge (Figure 3). In the second stage, we perform a tomographic inversion for the 2-D phase velocity variations across the study region, using a parameterization of 1120 nodes with the primary region of the inversion having a node spacing of 110 km. Two rows of nodes around the edges have a spacing of 220 km to more coarsely parameterize seismic structure outside of the primary study region (Figure 2a).

The inversion method solves for the 2-D phase velocities as spatially sampled at the location of the nodes. To produce a continuous phase velocity model, we perform Gaussian weighted spatial interpolation of the results [Forsyth and Li, 2005]. After making a number of tests, we chose a smoothing length of 240 km. Uncertainties in the derived phase velocity maps are quantified by plotting the standard errors calculated from the a posteriori model covariance matrix [Forsyth and Li, 2005].

3.3. Shear Velocity Inversion

3.3.1. Linear Inversion

We invert the phase velocity maps for a depth-dependent shear velocity structure using the approach described in Heeszel *et al.* [2013]. We first extract the phase velocity dispersion curve at each node and perform a linear inversion to determine the least squares best fit shear velocity [Herrmann and Ammon, 2002]

and then conduct a Monte Carlo resampling around the linear solution to find the best model (section 3.3.2). The ice layer thickness is fixed using Bedmap2 [Fretwell *et al.*, 2013].

Crustal thicknesses for the linear inversion are taken from a crustal thickness map of Antarctica determined from the inversion of short period Rayleigh wave phase and group velocities derived from noise correlation data [Sun *et al.*, 2013]. Crustal thicknesses from receiver functions alone are subject to errors caused by the use of inappropriate crustal velocity models [e.g., Schulte-Pelkum and Ben-Zion, 2012], so the use of noise correlation data results in more robust estimates. The Sun *et al.* [2013] model used crustal thickness estimates from receiver functions to define a smoothed map of crustal thickness as a starting model [Winberry and Anandakrishnan, 2004; Reading, 2006; Lawrence *et al.*, 2006a; Hansen *et al.*, 2009, 2010; Finotello *et al.*, 2011; Chaput *et al.*, 2014]. A higher-resolution crustal thickness map was then constructed from a linearized inversion of phase and group velocities, with the Moho velocity defined by comparing the shear velocity structure with the receiver function constraints. Finally, a Monte Carlo simulation was run to explore the trade-off between velocities in the lower crust/upper mantle and the total crustal thickness.

The crust in the linearized inversion is parameterized by three layers, with a thin upper crust (one eighth of the total thickness), a thicker middle crust (three eighths of the total thickness), and a lower crust (one half of the total thickness). The uppermost 100 km of the mantle is parameterized by 10 km thick layers, and the next 80 km is divided into 20 km thick layers. The remainder of the model is divided into 40 km thick layers down to a depth of 400 km. Since the *P* wave velocity has much less influence on the phase velocities than the shear velocity, we set the *P* velocity assuming V_p/V_s ratios of 1.73 for the crust and 1.81 for the upper mantle. We use different starting models for nodes located in East and West Antarctica (Figure 3b). The starting model for each region is the mean model that results from a linear shear velocity inversion and Monte Carlo resampling of the average phase velocity result for each region (Figure 3b).

3.3.2. Monte Carlo Inversion

Because there is a trade-off between upper mantle velocity and crustal thickness, and the crustal thickness must be assumed a priori in the linearized inversion, we perform Monte Carlo modeling of the shear velocity inversion results. The use of forward sampling techniques for exploring the model space is an increasingly common approach [e.g., Shapiro and Ritzwoller, 2002; Sambridge and Mosegaard, 2002; Shen *et al.*, 2012]. Here we apply the method of Heeszel *et al.* [2013] to perform Monte Carlo modeling, which performs a random walk around the initial model to generate a number of acceptable shear velocity models that fit the phase velocity results within an acceptable level of uncertainty. We parameterize the crustal layers in the same manner as in the linear inversion and allow the velocity to vary by 5%, while fixing the velocity of the ice layer. Layer thicknesses are also fixed, with the exception of the lower crustal and the uppermost mantle layer which are allowed to vary by up to ± 5 km. Shear velocities in the mantle are allowed to vary by up to 7% in the upper 200 km and 3% in the depth range of 200–280 km. We search the model space around the linear inverse solution, seeking to minimize the cost (C) in equation (1) below

$$C = \chi_{\text{red}}^2 \sqrt{\text{ISE}} \quad (1)$$

$$\chi_{\text{red}}^2 = \frac{1}{N} \sum_N^n \frac{(d_i^{\text{obs}} - d_i^{\text{pred}})^2}{(\sigma_i^{\text{obs}})^2} \quad (2)$$

$$\text{ISE} = \sum_{j=2}^{m-1} \left(\left[\frac{\Delta v_j^{j+1} - \Delta v_{j-1}^j}{\Delta z_j^{j+1} - \Delta z_{j-1}^j} \right]_{\text{forward}} - \left[\frac{\Delta v_j^{j+1} - \Delta v_{j-1}^j}{\Delta z_j^{j+1} - \Delta z_{j-1}^j} \right]_{\text{inverse}} \right)^2 \quad (3)$$

In the above equations, χ^2 is the reduced chi-square misfit determined by summing the misfit between observed and predicted phase velocities (d) over the observed standard deviation (σ), and ISE is a measure of model roughness determined by comparing the velocity change between layers in the forward and inverse models [Heeszel *et al.*, 2013]. Because individual layers of the model are not independently resolved, it is possible for models with excessive oscillations of the velocity structure to fit the data within an acceptable level of misfit, so we apply the ISE cost function to penalize models with large velocity jumps between mantle layers in order to ensure that nonphysical models (i.e., models with oscillating velocity reversals) are not included as acceptable models. The ISE metric is not applied to the crust or to the Moho discontinuity,

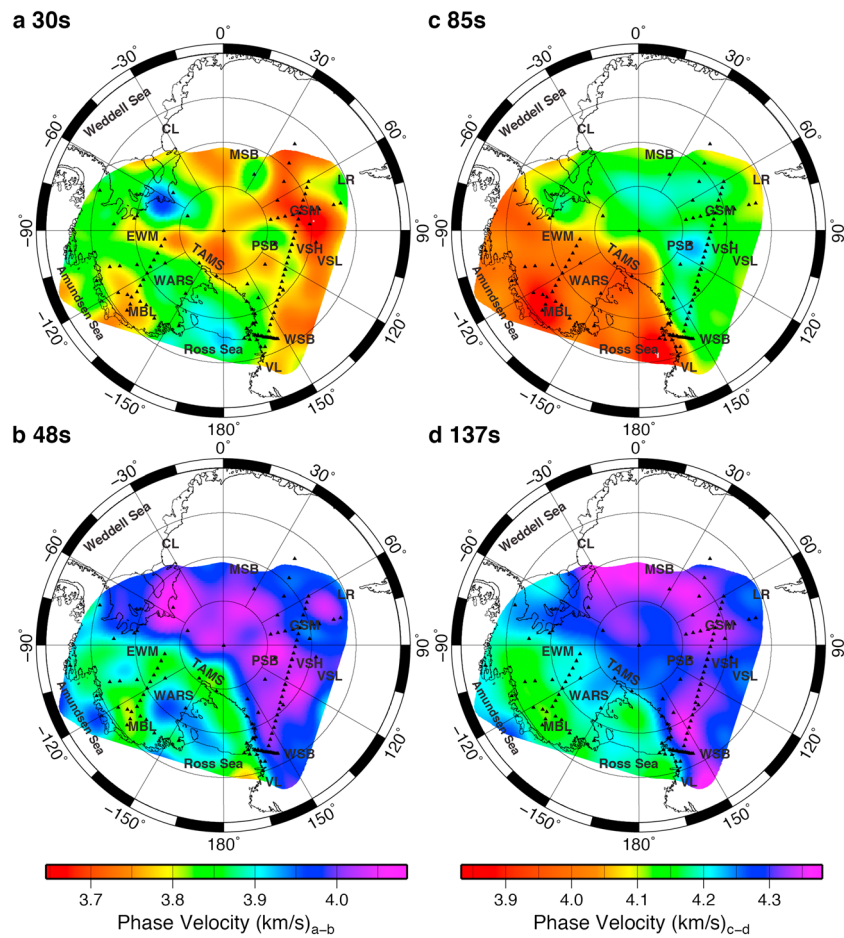


Figure 4. Phase velocity maps at (a) 30, (b) 48, (c) 85, and (d) 137 s. Stations are shown by black triangles, and labels are the same as in other figures. Color scale for Figures 4a and 4b is shown at the lower left, and color scale for Figures 4c and 4d at the lower right. Areas with poor resolution, as defined by standard error maps (Figure 5), are masked. West Antarctica transitions from being faster than East Antarctica at 30 s period (Figure 4a) to being slower at longer periods.

where such large velocity discontinuities are expected. If a model falls within the corridor of acceptable models, we include it in our mean model and uncertainty estimates. To limit the effect of varying V_p or density on the models, we fix V_p/V_s and density in the forward models to values in the linear inverse model.

The mean and median velocity models are determined by the Monte Carlo sampling smooth structure vertically because they represent an ensemble of all acceptable models. These vertically smooth models represent important statistical points within the model space but do not accurately represent our best estimate of the amount of variability within the Earth. They may also be biased toward the linear model, since the Monte Carlo perturbations in the sampling are centered on the linear model. To avoid these limitations in our interpretation, we utilize the best fit (lowest cost) model for constructing the preferred model. Because each node is sampled independently, we apply the same Gaussian horizontal smoothing parameters to the shear wave velocity models as we do to the phase velocity inversions to limit the introduction of poorly constrained horizontal roughness into the final shear velocity model and to ensure that features in the final model are consistent with the estimated spatial resolution of the data [Heeszel et al., 2013].

4. Results

4.1. Phase velocities

The results of the 2-D phase velocity tomography show large and well-resolved variability in structure across the study region (Figure 4). Standard error maps (Figure 5) reveal that lateral resolution across the study area is good. We clip all maps at the 0.04 km/s standard error contour at 85 s period for interpretation purposes.

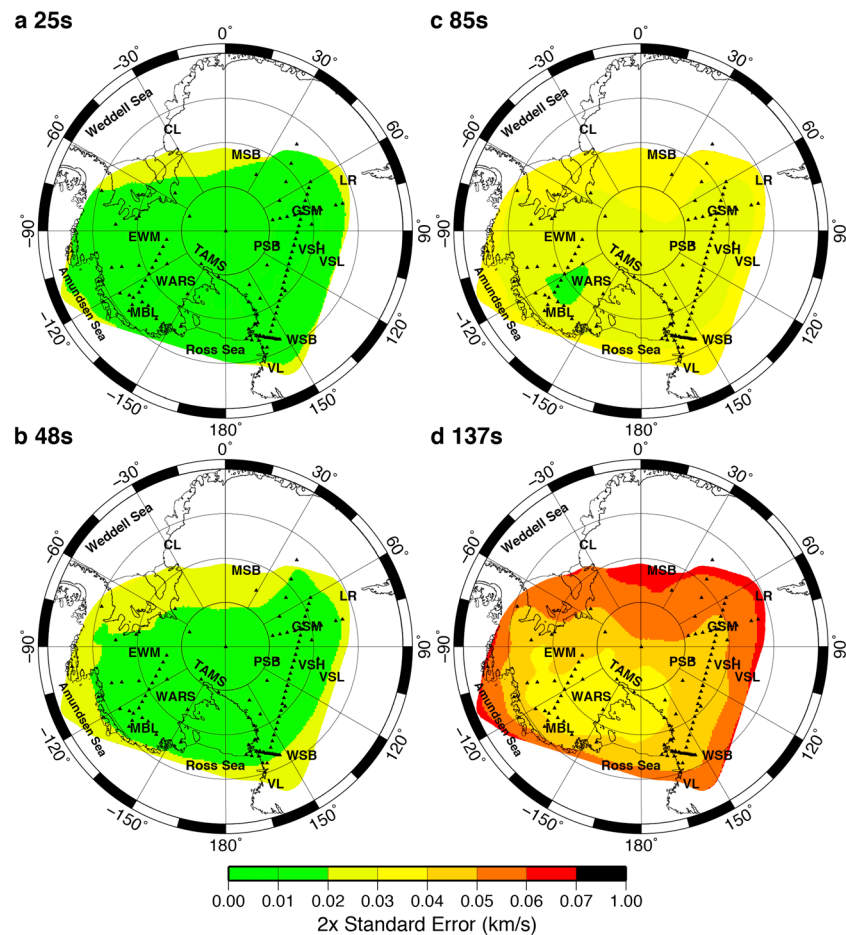


Figure 5. A posteriori standard error plot at different periods for the 2-D phase velocity inversion. Labels are the same as in Figure 1.

Slow phase velocities characterize East Antarctica relative to West Antarctica at periods of 20–30 s (Figure 4a). At these periods phase velocities are highly sensitive to crustal thickness, and slower velocities are indicative of regions with thicker crust. Prominent slow phase velocities are localized beneath the Gamburtsev Subglacial Mountains (GSM), where previous receiver functions, gravity, and surface wave studies indicate crustal thickness greater than 50 km [Hansen et al., 2010; Ferraccioli et al., 2011; Heeszel et al., 2013].

At longer periods for which phase velocities sample mantle depths, we observe velocities that are faster than the 1-D average model in the interior of East Antarctica. Due to the smoothing length (240 km) required in assembling this geographically extensive model, we are unable to image the East Antarctic craton with as high resolution as obtained in the Heeszel et al. [2013] study, which focused on East Antarctica using only data from the array of seismic stations surrounding the GSM. Thus, we will focus most of our discussion on West Antarctica, which has not been previously imaged with surface wave phase velocity tomography using local stations.

The phase velocity tomography shows that West Antarctica has a structure that is much different from East Antarctica. The shortest period observations (18–30 s) have significantly faster phase velocities compared to East Antarctica (Figure 4a). This is consistent with the region's thinner crust [Winberry and Anandakrishnan, 2004; Chaput et al., 2014] due to extension during the Mesozoic and Cenozoic [Cande et al., 2000; Siddoway et al., 2004; Siddoway, 2008; Wilson and Luyendyk, 2009; Granot et al., 2010]. At longer periods (Figures 4b–4d), phase velocities in West Antarctica are consistently slower than global averages and much slower than those in East Antarctica. Slow-velocity anomalies are concentrated beneath Marie Byrd Land, Ross Island, and in the Ross Sea region, extending inland toward the Central Transantarctic

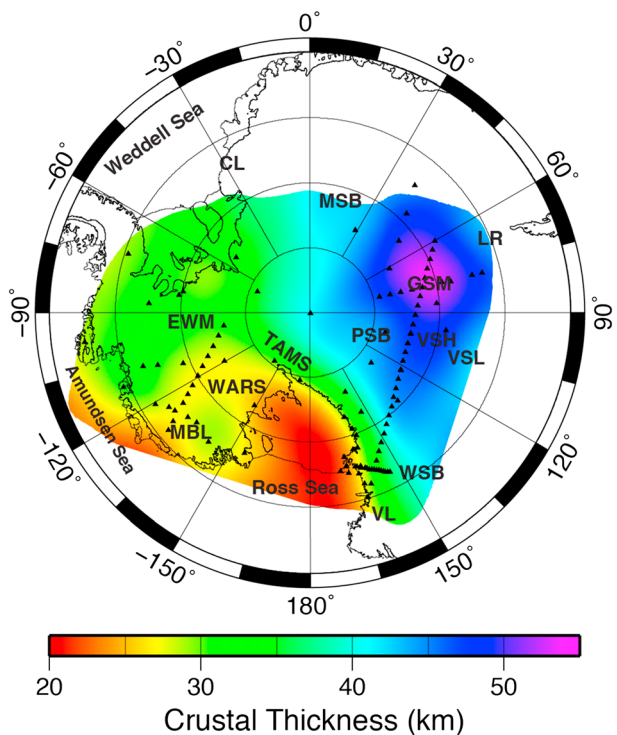


Figure 6. Map of crustal thicknesses resulting from the Monte Carlo inversion of surface wave velocities. Seismic station locations are shown as black triangles, and labels are the same as in Figure 1.

Mountains. These relatively narrow phase velocity anomalies appear to broaden with increasing period (Figure 4d). At the longest periods (>100 s) anomalous slow-velocity structure is centered beneath Marie Byrd Land.

4.2. Shear Velocities

Moho depths determined by the Monte Carlo inversion are shown in Figure 6. In most regions Moho depths do not deviate significantly from the a priori Moho depths based on the receiver function and noise correlation results. Thus, the surface wave data are generally well fit by the previous estimates. Although crustal velocities are solved for by both the linear and the Monte Carlo inversions, the resulting velocities are generally not well constrained. Since the mean West Antarctic crustal thickness is only about 25 km, Rayleigh wave phase velocities from periods shorter than 18 s, the minimum period of teleseismic surface wave studies, would be required to develop good crustal models. In addition, the crustal layers used in the inversions were fixed to rather arbitrary thicknesses. Therefore, we do not interpret or discuss the crustal model further.

Upper mantle velocity structure (Figure 7) shows the exceptionally strong velocity contrast between East and West Antarctica throughout the entire depth of good resolution. The high-velocity continental lithosphere of the East Antarctic craton extends to depths greater than 220 km (Figure 7d). West Antarctica is characterized by slower mantle velocities, with the exception of the region between the Ellsworth-Whitmore Mountains and Coats Land. Prominent upper mantle slow-velocity anomalies are centered on Ross Island and the Terror Rift, the Marie Byrd Land dome, and the Central TAMS, extending to at least 200 km depth (Figure 7c). Cross-section plots show that the West Antarctic slow-velocity anomalies lie beneath a high-velocity lithosphere of variable thickness (Figure 8). Spatial resolution becomes limited at 220 km depth, but the slowest velocities become centered beneath the Marie Byrd Land dome.

5. Discussion

5.1. East Antarctic Craton

The East Antarctic craton is defined by fast seismic velocities to depths of greater than 200 km throughout the region (Figure 7d). The velocity anomalies in this region are consistent with the bulk of East Antarctica being composed of Archean/Paleoproterozoic crustal blocks that were assembled during the Precambrian [Elliot, 1975; Dalziel, 1991; Boger *et al.*, 2001; Fitzsimons, 2000a, 2000b, 2003; Goodge *et al.*, 2010; Goodge and Finn, 2010; Boger, 2011]. A cross section extending from the southward extension of the Lambert Rift System (RFS) across the Gamburtsev Subglacial Mountains (GSM) and Wilkes Subglacial Basin and terminating in the Ross Sea region (Figure 8a) shows high mantle seismic velocities and thick crust underlying much of the craton. The region of greatest lithospheric thickness extends across the GSM and generally correlates with the thickest crust and the highest elevations. A more detailed, higher-resolution study of the surface wave structure of central East Antarctica as well as further discussion is presented in Heeszel *et al.* [2013].

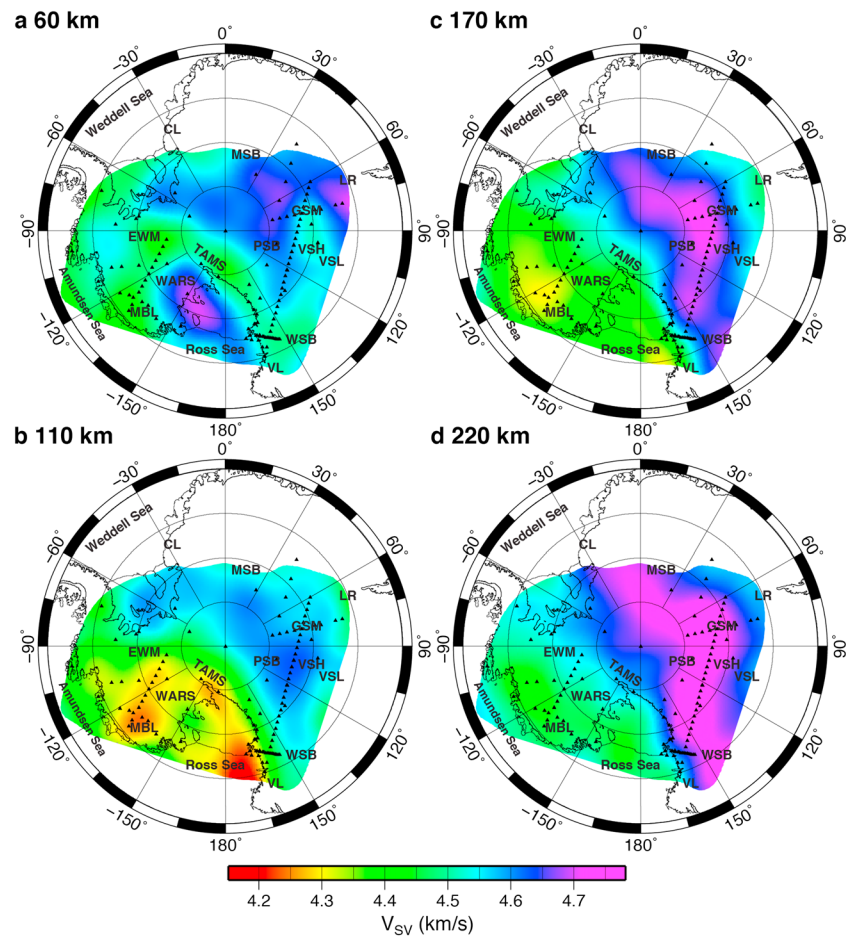


Figure 7. Shear velocity maps at depths of (a) 60, (b) 110, (c) 170, and (d) 220 km. Labels are same as in Figure 1. Areas with poor resolution, as defined by standard error maps (Figure 5), are masked.

5.2. Thermal Anomalies Beneath the Transantarctic Mountains and the Western Ross Sea

A region of slow seismic velocity in the upper mantle (60–120 km depth) follows the TAMS from the Ross Island region through the central TAMS and joins another slow-velocity anomaly extending across the WARS near the Whitmore Mountains. Watson *et al.* [2006] and Lawrence *et al.* [2006a, 2006b, 2006c] noted low velocities and high attenuation in the Ross Island region of their studies and attributed it to an upper mantle thermal anomaly. However, due to the limited extent of the array across the Ross Embayment, they were unable resolve the structure fully or comment on its lateral extent. The results in this study suggest that the anomaly occurs along the entire TAM front from the Ross Island region to the Ellsworth-Whitmore Mountains. This alignment of slow velocities follows the approximate trace of thin crustal thicknesses along the Terror Rift astride the flank of the TAMS, representing the youngest lithosphere in the Ross Sea [Wilson and Luyendyk, 2009]. Although extension along the Terror rift initiated at 17 Ma, GPS measurements and the absence of significant seismicity suggest that it is currently relatively inactive [Henrys *et al.*, 2007; Fielding *et al.*, 2008]. Thus, the slow-velocity anomaly in this region may represent a residual area of elevated temperatures in the upper mantle along the TAMS side of the Ross Sea remaining from the Miocene to recent extensional tectonism. This is consistent with the modeling of Huerta and Harry [2007], who found evidence for a progression from diffuse extension early in Ross Sea history to focused extension near the TAM front and the boundary between East and West Antarctica during the most recent extensional phase.

The slow-velocity anomaly along the TAM front does not vary significantly along the strike of the mountain front at 60 km depth, but the anomaly in the Ross Island region becomes much larger at greater depths and extends to at least 200 km (Figure 7). Resolution is reduced below 200 km, and it is difficult to determine

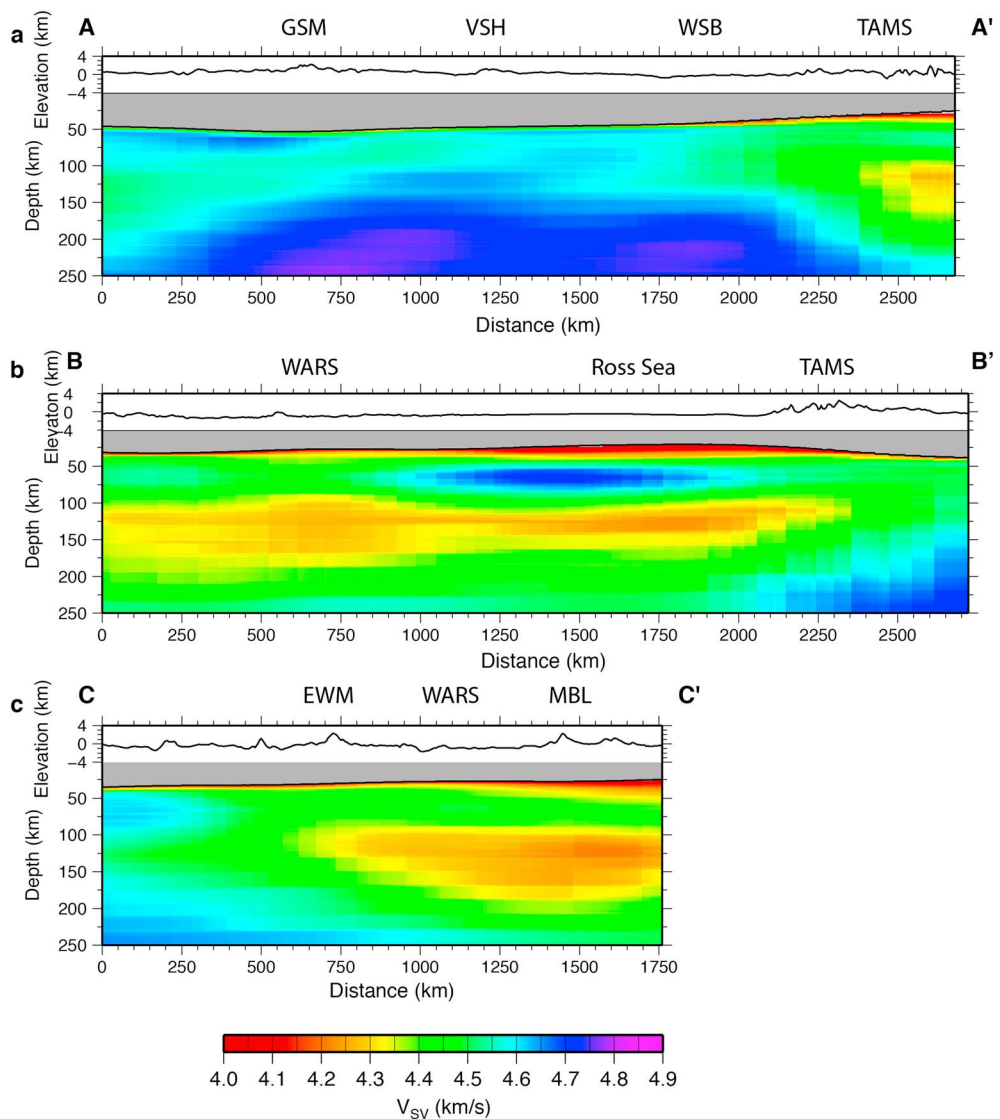


Figure 8. Seismic cross sections along the three lines shown in Figure 1. Geographical labels are the same as in Figure 1. (a) A-A' parallels the long line of TAMSEIS and AGAP/GAMSEIS seismic stations from the Ross Sea coast across the Gamburtsev Subglacial Mountains. (b) B-B' extends from the Amundsen Sea across the West Antarctic Rift System and the Ross Sea to the Transantarctic Mountains. (c) C-C' parallels the line of POLENET/ANET stations from the Marie Byrd Land coast across the Whitmore Mountains. Topography from Fretwell *et al.* [2013] is shown along the top. Crustal structure is not interpreted here.

whether the anomaly extends deeper. This anomaly is in agreement with previous results showing slow seismic velocity anomalies beneath Ross Island [Sieminski *et al.*, 2003; Watson *et al.*, 2006; Lawrence *et al.*, 2006a, 2006b; Hansen *et al.*, 2014]. The results here are consistent with the suggestion that active and recent volcanism in this region results from a mantle plume [e.g., Kyle *et al.*, 1992], since the inferred thermal anomaly in the upper 200 km is larger than in surrounding regions. However, the full depth extent of this feature is unknown, and studies of transition zone thickness do not show a thinning in this region, as would be expected for a mantle plume extending into the lower mantle [Reusch *et al.*, 2008; Emry *et al.*, 2015].

The central to southern TAMS near 86°S, 160°W show larger uppermost mantle velocity anomalies extending farther into East Antarctica than elsewhere along the TAMS (Figures 4c and 7b). Block *et al.* [2009] and O'Donnell and Nyblade [2014] estimated crustal thicknesses in excess of 45 km in the region based on satellite gravity lows, indicating a mass deficit in this region. However, receiver function crustal thickness estimates

clearly show thinner crustal thickness in this region [Chaput *et al.*, 2014], indicating that the mass deficit does not result from a thick crustal root. The mantle structure imaged in this study shows very slow mantle velocities extending to 140 km depth. This velocity anomaly, combined with the mass deficit observations from gravity suggest a thermal anomaly located in the upper mantle extending into East Antarctica. This region is also notable as the only location along the entire TAMS with late Cenozoic volcanism located on the East Antarctic side of the mountain range (Mount Early) [Stump *et al.*, 1980; LeMasurier, 1990].

There are two possible interpretations for the broad upper mantle anomaly extending into East Antarctica in the central TAMS. One possibility is that the extension was relatively concentrated in the Terror Rift area near Ross Island and at other regions along the TAM front in the Ross Sea area but becomes more diffuse and extended into East Antarctica in the central TAMS region, modifying and reheating the lithosphere in this region. Maximum K-Ar ages of volcanics in the area of Mount Early range from 15 to 19 Ma [Stump *et al.*, 1980] or approximately the same time as extension initiated on the Terror Rift, suggesting the thermal anomaly in this area formed at the same time as the initiation of early Miocene rifting.

An alternative model suggests that the anomalous area of the central TAMS, characterized by high elevations, strong slow mantle velocity anomaly extending into East Antarctica, Cenozoic volcanism, and observed mass deficit in the gravity data, represents a region of lithospheric delamination or destruction. Removal of old, cold continental lithosphere and replacement with warmer asthenospheric material have been associated with uplift and mountain building in several regions [Zandt *et al.*, 2004; Frassetto *et al.*, 2011; Bezada *et al.*, 2014]. The location of the anomaly at depths of 70–140 km is consistent with the replacement of continental lithosphere by warm asthenosphere around 17 Ma, further supporting this model.

5.3. Lithospheric Structure and Heat Flow of the West Antarctic Rift System

The WARS is characterized by a mantle lid of faster seismic velocities ($V_s \sim 4.4\text{--}4.7 \text{ km/s}$) extending to depths of 70–100 km, underlain by slower velocities ($V_s \sim 4.2\text{--}4.3 \text{ km/s}$) to depths of at least 180 km (Figures 7–8). In the low-velocity zone, the slowest anomalies extend across the central WARS, merging with the slow anomalies along the TAM front at the Whitmore Mountains to the south and with the large anomaly beneath the Marie Byrd Land (MBL) dome to the north. We interpret the low velocities as indicating a thermal anomaly in the upper mantle, representing thermally perturbed mantle from Mesozoic through Cenozoic extension in the WARS [Siddoway, 2008; Wilson and Luyendyk, 2009; Granot *et al.*, 2010].

We interpret the higher-velocity seismic lid as the seismological expression of a mantle lithosphere of variable thickness, consistent with gravity modeling near the TAM front [Huerta, 2007]. The central WARS between MBL and Ellsworth-Whitmore Mountains (EWM) shows slower lid velocities and inferred lithospheric thicknesses of about 70 km, whereas the eastern Ross Sea coastal regions show faster lid velocities and lithospheric thicknesses of up to 100 km (Figure 8b). The eastern Ross Sea and adjacent coast is thought to be the site of the oldest extension in the region, with ages of approximately 100–70 Ma [Wilson and Luyendyk, 2009], so that the thicker and faster lithosphere is consistent with significant cooling of the lithosphere since the cessation of tectonic activity inferred for this area.

There has been considerable discussion about the possibility of high geothermal heat flow in West Antarctica and its probable effects on the West Antarctic Ice Sheet [Pollard *et al.*, 2005; Vogel and Tulaczyk, 2006; Larour *et al.*, 2012]. However, the heat flow is poorly constrained by existing measurements and modeling. High heat flow has been estimated from the WAIS ice core [Clow *et al.*, 2012], and a recent heat flow measurement from beneath Subglacial Lake Whillans estimated an extremely high flux of $285 \pm 85 \text{ mW/m}^2$ [Fisher *et al.*, 2015]. Radar observations of subglacial water along with a hydrologic model suggest an average geothermal flux of about 115 mW/m^2 in the Thwaites Glacier catchment [Schroeder *et al.*, 2014]. Earlier estimates of the average heat flow of West Antarctica from lower resolution seismic studies suggest heat flow of $100\text{--}125 \text{ mW/m}^2$ for central west Antarctica [Shapiro and Ritzwoller, 2004], although estimates based on the depth of the Curie isotherm from satellite magnetic studies are much less [Maule *et al.*, 2005].

The presence of a thin but significant lithosphere places an upper bound on the average heat flow estimated in the WARS and MBL. A rough steady state calculation can be made assuming that the bottom of the lithosphere represents the intersection of a mantle adiabat with a conductive cooling thermal gradient in the lithosphere, assuming average values of crustal heat generation. Such calculations suggest that lithosphere thicknesses of 70 km are compatible with surface geothermal heat flow values of $70\text{--}80 \text{ mW/m}^2$, whereas

thicknesses of 100 km correspond to heat flow of 60–70 mW/m² (see for example Figure 3 in *Lee et al.* [2011]). The latter estimate corresponds well with the measured heat flow of 69 mW/m² measured from the Siple Dome drill core near the east coast of the Ross Sea [*Engelhardt*, 2004], where we find thicker lithosphere. Conversely, the observed lithospheric thicknesses are incompatible with the highest heat flow measurements. It is possible that the geothermal gradient beneath the WARS is not steady state, with the lower lithosphere recently undergoing large-scale heating, for example, by asthenospheric flow from an MBL plume. However, in this case there would have been insufficient time for the high heat flow from the recent alteration of the lower lithosphere to propagate to the surface. For recent activity (within the last ~10 Ma), only very shallow perturbations will be expressed as increased surface heat flow, and the presence of the lithosphere shows that such shallow thermal perturbations have not occurred over large regions. Thus, allowing for reasonable uncertainties in the various parameters, we can estimate the maximum possible geothermal heat flow averaged over large regions of the WARS to be about 90 mW/m².

While the above provides an estimate of average regional heat flux, there is also a variety of evidence for locally higher geothermal heat flow beneath the WARS, including heat flow measurements [*Clow et al.*, 2012; *Fisher et al.*, 2015], estimates from aerogeophysics [*Schroeder et al.*, 2014], and evidence of recent subglacial and active intracrustal magmatism [e.g., *Blankenship et al.*, 1993; *Behrendt et al.*, 1994; *Lough et al.*, 2013]. Because of the large smoothing length of long period Rayleigh waves, this study lacks the resolution to resolve small regions of thermally perturbed lithosphere that may correspond to limited Neogene extensional activity. A recent body wave tomographic study [*Lloyd et al.*, 2015] with higher spatial resolution but reduced depth resolution across West Antarctica inferred a geographically limited mantle thermal anomaly associated with the Bentley Trench and associated crustal thinning [*Chaput et al.*, 2014] just north of the EWM and suggested it corresponded to a limited Neogene extension event coincident with the Terror Rift in the Ross Sea region [*Henrys et al.*, 2007; *Fielding et al.*, 2008; *Granot et al.*, 2010]. Thus, isolated measurements of high heat flow may indicate localized areas of recent tectonic activity. Higher-resolution seismic models mapping the upper mantle structure of West Antarctica will be required to provide better constraints on mantle thermal structure and the regional variation of heat flow on smaller spatial scale lengths.

5.4. The Ellsworth-Whitmore Mountains: A Distinct Province of Altered Precambrian Lithosphere

The Ellsworth-Whitmore Mountains (EWM) crustal block of West Antarctica is a region of Gondwana Precambrian cratonic margin crust that has been incorporated into West Antarctica [*Dalziel and Elliot*, 1982; *Grunow et al.*, 1987; *Randall and Mac Niocail*, 2004]. Rayleigh wave phase velocities in the region are well fit by crustal thicknesses greater than that of the WARS (Figure 6), consistent with crustal thicknesses of 30–37 km obtained from receiver functions [*Chaput et al.*, 2014], but much less than the 40–55 km thick crust found in the East Antarctic Craton [*Hansen et al.*, 2009, 2010; *An et al.*, 2015]. The results shown here indicate that the uppermost mantle structure of the region is also distinct from both the WARS and East Antarctica. The low asthenospheric velocities of the WARS are bounded by the EWM, and velocities at 100 km depth are about 4.4 km/s as compared to 4.25 km/s for the WARS and 4.6 km/s for East Antarctica (Figures 7b and 8c). Better spatial resolution of this region is provided by shear wave body wave tomography [*Lloyd et al.*, 2015], which shows a velocity transition along the POLENET/ANET line of seismographs occurs about 150 km north of the crest of the Whitmore Mountains, with mantle velocities at depths of 100–200 km beneath the Whitmore Mountains being about 4% higher than beneath the WARS, consistent with this study.

Our results are consistent with the interpretation of the EWM as a Precambrian terrain originally located between the East Antarctic and African cratons, as indicated by inferred Grenvillian age crustal basement [*Curtis et al.*, 1999]. The lithosphere was then significantly altered before or during Gondwana breakup when it was translated as a rotated into its current tectonic position [*Randall and Mac Niocail*, 2004]. The intermediate upper mantle velocities found in this study are consistent with a continental lithosphere block that has been significantly thinned or thermally altered during those tectonic events. However, the lithosphere is significantly thicker and cooler than lithosphere throughout most of the WARS, which has been thermally rejuvenated by much more recent Cretaceous through Neogene extension. It is also possible that although Grenvillian age rocks are exposed to the north of the Ellsworth Mountains, the basement between the Ellsworth and Whitmore Mountains may be early Paleozoic Ross orogen magmatic arc rocks, with inherently thinner and less distinctive lithospheric velocity and thickness.

5.5. A Mantle Thermal Anomaly Beneath the Marie Byrd Land Dome

The largest slow mantle velocity anomaly in this study is located at depths of 80–200 km beneath the Marie Byrd Land dome, an area of high topography and volcanism. The velocity anomaly is centered on the Executive Committee Range, which is at the center of the topographic anomaly and is notable for prominent volcanoes, including the highest volcano in Antarctica (Mount Sidley; active until 4.2 Ma) [Panter *et al.*, 1997] and recently detected intracrustal magmatic activity [Lough *et al.*, 2013]. We interpret the strong slow-velocity anomalies as indicating a major upper mantle thermal anomaly. This thermal anomaly supports the topographic elevation of the dome, as is indicated by isostatic calculations that show the observed crustal thicknesses of around 30 km, while several kilometers thicker than the central WARS are insufficient to isostatically support the topography [Chaput *et al.*, 2014], thus requiring support from low-density mantle.

Some previous studies have attributed the topography and volcanism of MBL to a mantle plume [LeMasurier and Landis, 1996], and Sr, Nd, and Pb isotopic analyses of lava compositions show a plume affinity [Panter *et al.*, 1997]. The thermal anomaly imaged in this study extends deeper below MBL than in the WARS or elsewhere in Antarctica, but resolution in our model is reduced at depths greater than 200 km, so it is difficult to determine how deep the thermal anomaly extends. Regional body wave tomography suggests the anomaly depths extend to at least 200–300 km [Lloyd *et al.*, 2015], but resolution is also reduced in those models due to the limited number of seismographs. Larger-scale *P* wave tomographic imaging suggests that the low-velocity anomaly has a complicated geometry and does not extend into the transition zone immediately beneath MBL [Hansen *et al.*, 2014]. This is consistent with transition zone thickness measurements, which do not show the thinning expected for elevated transition zone temperatures directly below this region but rather show thinning in adjacent coastal regions [Emry *et al.*, 2015]. Possible mantle plumes may be difficult to image in the transition zone and the midmantle due to the fact that a plume conduit could be a much narrower and more subtle feature compared to classical asthenospheric plume models, where the plume encounters the bottom of the lithosphere and spreads laterally, and where remnants of the plume head may persist for millions of years [Griffiths and Campbell, 1990; Ribe *et al.*, 2007]. Areas where subcontinental plume structures have been relatively well imaged (e.g., Yellowstone [Schmandt *et al.*, 2012] being one of the best examples) indicate that complex structure and heterogeneous deflection of mantle transition zone discontinuities can occur.

Acknowledgments

We would like to acknowledge the support of all the field teams associated with the collection of data presented here, particularly Patrick Shore as well as the polar support specialists at IRIS/PASSCAL. We thank the pilots of Kenn Borek Air and the New York Air Guard for flight support and the staff at AGAP-S camp, Byrd Camp, South Pole Station, and McMurdo Station for logistical support. We also thank two anonymous reviewers for their comments which significantly improved this paper. This research is supported by NSF grants ANT-0537597, ANT-0838934, ANT-0632209, and PLR-1246712. Seismic instrumentation was provided by the Incorporated Research Institutions for Seismology (IRIS) through the PASSCAL Instrument Center at New Mexico Tech. Data are available through the IRIS Data Management Center (<http://ds.iris.edu/ds/nodes/dmc/>). The facilities of the IRIS Consortium are supported by the National Science Foundation under Cooperative agreement EAR-1261681, the NSF Division of Polar Programs, and the DOE National Nuclear Security Administration. Figures in this work were produced in GMT [Wessel and Smith, 1994], and seismic processing was performed using the *seizmo* routines for processing SAC files in MATLAB® developed by G. Euler (<https://github.com/g2e/seizmo>).

6. Summary and Conclusions

We determine phase velocities from teleseismic Rayleigh waves and invert them to create a three-dimensional model of the Antarctic continent extending from the Gamburtsev Subglacial Mountains in East Antarctica to Marie Byrd Land and the Ellsworth-Whitmore Mountains crustal block in West Antarctica. East Antarctica is defined by a thick crust and fast lithospheric root extending to depths of ~250 km. In contrast, we find thin crust and slow mantle velocities consistent with regions of Mesozoic and Cenozoic extension and tectonism underlie most of West Antarctica. Slow upper mantle velocities at depths of 60–120 km depth follow the boundary of the Ross Sea and TAMS along the trace of the Terror Rift. A more regionally extensive slow upper mantle anomaly underlies Ross Island and Mount Erebus and may represent a mantle plume structure, although the depth extent below approximately 200 km is poorly constrained. A larger, shallower, anomaly is also found beneath the Central Transantarctic Mountains that extends some distance into East Antarctica, probably resulting from mid-Cenozoic lithospheric delamination.

The West Antarctic Rift System is underlain by a lithosphere with thickness varying from about 70 km to 100 km, with the thickest lithosphere found beneath the Eastern Ross Sea. This conductive lithosphere demonstrates that greatly elevated geothermal heat flow (greater than $\sim 90 \text{ mW/m}^2$) cannot be widespread across West Antarctica. The Ellsworth-Whitmore Mountains represent a Precambrian lithospheric block that has undergone thermal lithospheric modification. Marie Byrd Land shows slow mantle to depths of >200 km beneath the center of Marie Byrd Land that provide buoyant support for the high topography and may represent the uppermost extent of a complex plume structure imaged to greater depths in recent body wave tomography studies.

References

- Accardo, N. J., D. A. Wiens, S. Hernandez, R. C. Aster, A. Nyblade, A. Huerta, S. Anandakrishnan, T. Wilson, D. S. Heeszel, and I. W. D. Dalziel (2014), Upper mantle seismic anisotropy beneath the West Antarctic Rift System and surrounding region from shear wave splitting analysis, *Geophys. J. Int.*, 198, 414–429, doi:10.1093/gji/ggu117.

- An, M., D. A. Wiens, Y. Zhao, M. Feng, A. A. Nyblade, M. Kanao, Y. Li, A. Maggi, and J. J. Lévéque (2015), S-velocity model and inferred Moho topography beneath the Antarctic Plate from Rayleigh waves, *J. Geophys. Res. Solid Earth*, 120, 359–383, doi:10.1002/2014JB011332.
- Behrendt, J. C., D. D. Blankenship, C. A. Finn, R. E. Bell, R. E. Sweeney, S. M. Hodge, and J. M. Brozena (1994), Casertz aeromagnetic data reveal late Cenozoic flood basalts (?) in the West Antarctic Rift System, *Geology*, 22, 527–530.
- Bezada, M. J., E. D. Humphreys, J. M. Davila, and R. Carbonell (2014), Piecewise delamination of Moroccan lithosphere from beneath the Atlas Mountains, *Geochem. Geophys. Geosyst.*, 15, 975–985, doi:10.1002/2013GC005059.
- Blankenship, D. D., R. E. Bell, S. M. Hodge, J. M. Brozena, J. C. Behrendt, and C. A. Finn (1993), Active volcanism beneath the West Antarctic Ice Sheet and implications for ice-sheet stability, *Nature*, 361, 526–529.
- Block, A. E., R. E. Bell, and M. Studinger (2009), Antarctic crustal thickness from satellite gravity: Implications for the Transantarctic and Gamburtsev Subglacial Mountains, *Earth Planet. Sci. Lett.*, 288, 194–203, doi:10.1016/j.epsl.2009.09.022.
- Boger, S. D. (2011), Antarctica—Before and after Gondwana, *Precambrian Res.*, 19, 335–371, doi:10.1016/j.gr.2010.09.003.
- Boger, S. D., C. J. L. Wilson, and C. M. Fanning (2001), Early Paleozoic tectonism within the East Antarctic craton: The final suture between east and west Gondwana?, *Geology*, 29(5), 463–466, doi:10.1130/0091-7613(2001)029<0463:EPTWTE>2.0.CO;2.
- Cande, S. C., J. M. Stock, R. D. Müller, and T. Ishihara (2000), Cenozoic motion between East and West Antarctica, *Nature*, 404, 145–150, doi:10.1038/35004501.
- Chaput, J., R. C. Aster, A. Huerta, X. Sun, A. Lloyd, D. Wiens, A. Nyblade, S. Anandakrishnan, J. P. Winberry, and T. Wilson (2014), The crustal thickness of West Antarctica, *J. Geophys. Res. Solid Earth*, 119, 378–395, doi:10.1002/2013JB010642.
- Clow, G. D., K. M. Cuffey, and E. D. Waddington (2012), High heat-flow beneath the central portion of the West Antarctic ice sheet, In AGU Fall Meeting Abstracts (p. 0577).
- Cooper, A. K., and F. J. Davey (1985), Episodic rifting of Phanerozoic rocks in the Victoria Land Basin, western Ross Sea, Antarctica, *Science*, 229(4718), 1085–1087.
- Corr, H. F. J., and D. G. Vaughan (2008), A recent volcanic eruption beneath the West Antarctic ice sheet, *Nat. Geosci.*, 1, 122–125, doi:10.1038/ngeo106.
- Curtis, M. L., P. T. Leat, T. R. Riley, B. C. Storey, I. L. Millar, and D. E. Randall (1999), Middle Cambrian rift-related volcanism in the Ellsworth Mountains, Antarctica: Tectonic implications for the palaeo-Pacific margin of Gondwana, *Tectonophysics*, 304, 275–299.
- Dalziel, I. W. D. (1991), Pacific margins of Laurentia and East Antarctica-Australia as a conjugate rift pair: Evidence and implications for an Eocambrian supercontinent, *Geology*, 19, 598–601.
- Dalziel, I. W. D., and D. H. Elliot (1982), West Antarctica: Problem child of Gondwanaland, *Tectonics*, 1(1), 3–19.
- Danesi, S., and A. Morelli (2000), Group velocity of Rayleigh waves in the Antarctic region, *Phys. Earth Planet. Int.*, 122, 55–66, doi:10.1016/S0031-9201(00)00186-2.
- Danesi, S., and A. Morelli (2001), Structure of the upper mantle under the Antarctic Plate from surface wave tomography, *Geophys. Res. Lett.*, 28(23), 4395–4398.
- Davey, F. J., and G. Brancolini (1995), The late Mesozoic and Cenozoic structural setting of the Ross Sea region, *Antarct. Res. Ser.*, 68, 167–182.
- Davey, F. J., S. C. Cande, and J. M. Stock (2006), Extension in the western Ross Sea region-links between Adare Basin and Victoria Land Basin, *Geophys. Res. Lett.*, 33, L20315, doi:10.1029/2006GL027383.
- DiVenere, V. J., D. V. Kent, and I. W. D. Dalziel (1994), Mid-Cretaceous paleomagnetic results from Marie Byrd Land, West Antarctica: A test of post-100 Ma relative motion between East and West Antarctica, *J. Geophys. Res.*, 99(B8), 15,115–15,139.
- Dziewonski, A. M., and D. L. Anderson (1981), Preliminary reference Earth model, *Phys. Earth Planet. Inter.*, 25, 297–356.
- Elliot, D. H. (1975), Tectonics of Antarctica: A review, *Am. J. Sci.*, 275(A), 45–106.
- Emry, E. L., A. A. Nyblade, J. Julià, S. Anandakrishnan, R. C. Aster, D. A. Wiens, A. D. Huerta, and T. J. Wilson (2015), The mantle transition zone beneath West Antarctica: Seismic evidence for hydration and thermal upwellings, *Geochem. Geophys. Geosyst.*, 16, 40–58, doi:10.1002/2014GC005588.
- Engelhardt, H. (2004), Ice temperature and high geothermal flux at Siple Dome, West Antarctica, from borehole measurements, *J. Glaciol.*, 50, 251–256.
- Ferraccioli, F., E. Armadillo, T. Jordan, E. Bozzo, and H. Corr (2009), Aeromagnetic exploration over the East Antarctic Ice Sheet: A new view of the Wilkes Subglacial Basin, *Tectonophysics*, 478, 62–77, doi:10.1016/j.tecto.2009.03.013.
- Ferraccioli, F., C. A. Finn, T. A. Jordan, R. E. Bell, L. M. Anderson, and D. Damaske (2011), East Antarctic rifting triggers uplift of the Gamburtsev Mountains, *Nature*, 479, 388–392, doi:10.1038/nature10566.
- Fielding, C. R., J. Whittaker, S. A. Henrys, T. J. Wilson, and T. R. Naish (2008), Seismic facies and stratigraphy of the Cenozoic succession in McMurdo Sound, Antarctica: Implications for tectonic, climatic and glacial history, *Palaeogeogr. Palaeoclimatol. Palaeoecol.*, 260(1), 8–29.
- Finotello, M., A. Nyblade, J. Julia, D. A. Wiens, and S. Anandakrishnan (2011), Crustal V_p/V_s ratios and thickness for Ross Island and the Transantarctic Mountain front, Antarctica, *Geophys. J. Int.*, 185, 85–92, doi:10.1111/j.1365-246X.2011.04946.x.
- Fisher, A. T., K. D. Mankoff, S. M. Tulaczyk, S. W. Tyler, and N. Foley (2015), High geothermal heat flux measured below the West Antarctic Ice Sheet, *Sci. Adv.*, 1(6), e1500093, doi:10.1126/sciadv.1500093.
- Fitzsimons, I. C. W. (2000a), A review of tectonic events in the East Antarctic Shield and their implications for Gondwana and earlier supercontinents, *J. Afr. Earth Sci.*, 31(1), 3–23.
- Fitzsimons, I. C. W. (2000b), Grenville-age basement provinces in East Antarctica: Evidence for three separate collisional orogens, *Geology*, 28(10), 879–882, doi:10.1130/0091-7613(2000)28<879:GBPIEA>2.0.CO;2.
- Fitzsimons, I. C. W. (2003), Proterozoic basement provinces in southern and southwestern Australia, and their correlation with Antarctica, in *Proterozoic East Gondwana: Supercontinent Assembly and Breakup*, *Geol. Soc. London Spec. Publ.*, edited by M. Yoshida, B. F. Windley, and S. Dasgupta, pp. 93–130, London.
- Forsyth, D. W., and A. Li (2005), Array analysis of two-dimensional variations in surface wave phase velocity and azimuthal anisotropy in the presence of multipathing interference, in *Seismic Earth: Array Analysis of Broadband Seismograms*, edited by A. Levander and G. Nolet, pp. 81–97, AGU, Washington, D. C.
- Frassetto, A., G. Zandt, H. Gilbert, T. J. Owens, and C. H. Jones (2011), Lithospheric structure of the Sierra Nevada from receiver functions and implications for lithospheric foundering, *Geosphere*, 7, 898–921, doi:10.1130/GES00570.1.
- Fretwell, P., et al. (2013), Bedmap2: Improved ice bed, surface and thickness datasets for Antarctica, *Cryosphere*, 7, 375–393, doi:10.5194/tc-7-375-2013.
- Goodge, J. W., and C. M. Fanning (2010), Composition and age of the East Antarctic Shield in eastern Wilkes Land determined by proxy of Oligocene-Pleistocene glaciomarine sediment and Beacon Supergroup sandstones, Antarctica, *Geol. Soc. Am. Bull.*, 122, 1135–1159, doi:10.1130/B30079.1.

- Goodge, J. W., and C. A. Finn (2010), Glimpses of East Antarctica: Aeromagnetic and satellite magnetic view from the central Transantarctic Mountains of East Antarctica, *J. Geophys. Res.*, **115**, B09103, doi:10.1029/2009JB006890.
- Goodge, J. W., C. M. Fanning, and V. C. Bennett (2001), U-Pb evidence of ~1.7 Ga crustal tectonism during the Nimrod Orogeny in the Transantarctic Mountains, Antarctica: Implications for Proterozoic plate reconstructions, *Precambrian Res.*, **112**, 261–288.
- Goodge, J. W., C. M. Fanning, D. M. Brecke, K. J. Licht, and E. F. Palmer (2010), Continuation of the Laurentian Grenville Province across the Ross Sea Margin of East Antarctica, *J. Geol.*, **118**(6), 601–619, doi:10.1086/656385.
- Granot, R., S. C. Cande, J. M. Stock, F. J. Davey, and R. W. Clayton (2010), Postspreading rifting in the Adare Basin, Antarctica: Regional tectonic consequences, *Geochem. Geophys. Geosyst.*, **11**, Q08005, doi:10.1029/2010GC003105.
- Granot, R., S. C. Cande, J. M. Stock, and D. Damaske (2013), Revised Eocene-Oligocene kinematics for the West Antarctic rift system, *Geophys. Res. Lett.*, **40**, 279–284, doi:10.1029/2012GL054181.
- Griffiths, R. W., and I. H. Campbell (1990), Stirring and structure in mantle starting plumes, *Earth Planet. Sci. Lett.*, **99**, 66–78.
- Grunow, A. M., I. W. D. Dalziel, and D. V. Kent (1987), Ellsworth-Whitmore Mountains Crustal Block, Western Antarctica: New paleomagnetic results and their tectonic significance, in *Gondwana Six: Structure, Tectonics, and Geophysics*, pp. 161–171, AGU, Washington, D. C.
- Grunow, A. M., D. V. Kent, and I. W. D. Dalziel (1991), New paleomagnetic data from Thurston Island: Implications for the tectonics of West Antarctica and Weddell Sea opening, *J. Geophys. Res.*, **96**(B11), 17,935–17,954.
- Hansen, S. E., J. Julià, A. A. Nyblade, M. L. Pyle, D. A. Wiens, and S. Anandakrishnan (2009), Using S wave receiver functions to estimate crustal structure beneath ice sheets: An application to the Transantarctic Mountains and East Antarctic craton, *Geochem. Geophys. Geosyst.*, **10**, Q08014, doi:10.1029/2009GC002576.
- Hansen, S. E., A. A. Nyblade, D. S. Heeszel, D. A. Wiens, P. J. Shore, and M. Kanao (2010), Crustal structure of the Gamburtsev Mountains, East Antarctica, from S-wave receiver functions and Rayleigh wave phase velocities, *Earth Planet. Sci. Lett.*, **300**, 395–401, doi:10.1016/j.epsl.2010.10.022.
- Hansen, S. E., J. H. Graw, L. M. Kenyon, A. A. Nyblade, D. A. Wiens, R. C. Aster, A. D. Huerta, S. Anandakrishnan, and T. Wilson (2014), Imaging the Antarctic mantle using adaptively parameterized P-wave tomography: Evidence for heterogeneous structure beneath West Antarctica, *Earth Planet. Sci. Lett.*, **408**, 66–78.
- Heeszel, D. S., D. A. Wiens, A. A. Nyblade, S. E. Hansen, M. Kanao, M. An, and Y. Zhao (2013), Rayleigh wave constraints on the structure and tectonic history of the Gamburtsev Subglacial Mountains, East Antarctica, *J. Geophys. Res. Solid Earth*, **118**, 2138–2153, doi:10.1002/jgrb.50171.
- Henrys, S. A., T. J. Wilson, J. M. Whittaker, C. R. Fielding, J. M. Hall, and T. Naish (2007), Tectonic history of mid-Miocene to present southern Victoria Land Basin, inferred from seismic stratigraphy in McMurdo Sound, Antarctica, in *Antarctica: A Keystone in a Changing World – Online Proceedings of the 10th ISAES*, U.S. Geol. Surv. Open File Rep. 2007-1047, Short Res. Pap. 049, edited by A. K. Cooper et al., 4 pp., doi:10.3133/of2007-1047.srp049.
- Herrmann, R. B., and C. J. Ammon (2002), *Computer Programs in Seismology: Surface Waves, Receiver Functions and Crustal Structure*, 110 pp., St. Louis Univ, St. Louis, Mo.
- Hole, M. J., and W. E. LeMasurier (1994), Tectonic controls on the geochemical composition of Cenozoic, mafic alkaline volcanic rocks from West Antarctica, *Contrib. Mineral. Petrol.*, **117**, 187–202.
- Huerta, A. D. (2007), Lithospheric structure across the Transantarctic Mountains constrained by an analysis of gravity and thermal structure, in *Antarctica: A Keystone in a Changing World*, U.S. Geol. Surv. Open File Rep. 2007-1047, edited by A. K. Cooper and C. R. Raymond, pp. 1–4, U.S. Geol. Surv., Reston, Va.
- Huerta, A. D., and D. L. Harry (2007), The transition from diffuse to focused extension: Modeled evolution of the West Antarctic Rift system, *Earth Planet. Sci. Lett.*, **255**, 133–147, doi:10.1016/j.epsl.2006.12.011.
- Ivins, E. R., and C. G. Sammis (1995), On lateral viscosity contrast in the mantle and the rheology of low frequency geodynamics, *Geophys. J. Int.*, **123**, 305–322.
- Jankowski, E. J., and D. J. Drewry (1981), The structure of West Antarctica from geophysical studies, *Nature*, **291**, 17–21, doi:10.1038/291017a0.
- Jordan, T. A., F. Ferraccioli, D. G. Vaughan, J. W. Holt, H. Corr, D. D. Blankenship, and T. M. Diehl (2010), Aerogravity evidence for major crustal thinning under the Pine Island Glacier region (West Antarctica), *Geol. Soc. Am. Bull.*, **122**(5–6), 714–726.
- Kyle, P. R., J. A. Moore, and M. F. Thirlwall (1992), Petrologic evolution of anorthoclase phonolite lavas at Mount Erebus, Ross Island, Antarctica, *J. Petrol.*, **33**, 849–875.
- Larour, E., M. Morlighem, H. Seroussi, J. Schiermeier, and E. Rignot (2012), Ice flow sensitivity to geothermal heat flux of Pine Island Glacier, Antarctica, *J. Geophys. Res.*, **117**, F04023, doi:10.1029/2012JF002371.
- Lawrence, J. F., D. A. Wiens, A. A. Nyblade, S. Anandakrishnan, P. J. Shore, and D. Voigt (2006a), Crust and upper mantle structure of the Transantarctic Mountains and surrounding regions from receiver functions, surface waves, and gravity: Implications for uplift models, *Geochem. Geophys. Geosyst.*, **7**, Q10011, doi:10.1029/2006GC001282.
- Lawrence, J. F., D. A. Wiens, A. A. Nyblade, S. Anandakrishnan, P. J. Shore, and D. Voigt (2006b), Upper mantle thermal variations beneath the Transantarctic Mountains inferred from teleseismic S-wave attenuation, *Geophys. Res. Lett.*, **33**, L03303, doi:10.1029/2005GL024516.
- Lawrence, J. F., D. A. Wiens, A. A. Nyblade, S. Anandakrishnan, P. J. Shore, and D. Voigt (2006c), Rayleigh wave phase velocity analysis of the Ross Sea, Transantarctic Mountains, and East Antarctica from a temporary seismograph array, *J. Geophys. Res.*, **111**, B06302, doi:10.1029/2005JB003812.
- Lee, C.-T. A., P. Luffi, and E. J. Chin (2011), Building and destroying continental mantle, *Ann Rev. Earth Planet. Sci.*, **39**, 59–90.
- LeMasurier, W. E. (1990), Late Cenozoic volcanism on the Antarctic Plate, in *Volcanoes of the Antarctic Plate and Southern Oceans*, Antarct. Res. Ser., vol. 48, edited by W. E. LeMasurier and J. W. Thomson, AGU, Washington, D. C.
- LeMasurier, W. E., and C. A. Landis (1996), Mantle-plume activity recorded by low-relief erosion surfaces in West Antarctica and New Zealand, *Geol. Soc. Am. Bull.*, **108**, 1450–1466, doi:10.1130/0016-7606.
- Li, A., D. W. Forsyth, and K. M. Fischer (2003), Shear velocity structure and azimuthal anisotropy beneath eastern North America from Rayleigh wave inversion, *J. Geophys. Res.*, **108**(B8), 2362, doi: 10.1029/2002JB002259.
- Lloyd, A. J., A. A. Nyblade, D. A. Wiens, S. E. Hansen, M. Kanao, P. J. Shore, and D. Zhao (2013), Upper mantle seismic structure beneath central East Antarctica from body wave tomography: Implications for the origin of the Gamburtsev Subglacial Mountains, *Geochem. Geophys. Geosyst.*, **14**, 902–920, doi:10.1002/ggge.20098.
- Lloyd, A. J., D. A. Wiens, A. A. Nyblade, S. Anandakrishnan, R. C. Aster, A. D. Huerta, T. J. Wilson, I. W. D. Dalziel, P. J. Shore, and D. Zhao (2015), A seismic transect across West Antarctica: Evidence for mantle thermal anomalies beneath the Bentley Subglacial Trench and the Marie Byrd Land Dome, *J. Geophys. Res. Solid Earth*, **120**, 8439–8460.
- Lough, A. C., D. A. Wiens, C. G. Barcheck, S. Anandakrishnan, R. C. Aster, D. D. Blankenship, A. D. Huerta, A. Nyblade, D. A. Young, and T. J. Wilson (2013), Seismic detection of an active subglacial magmatic complex in Marie Byrd Land, Antarctica, *Nat. Geosci.*, **6**, 1031–1035, doi:10.1038/ngeo1992.

- Maule, C. F., M. E. Purucker, N. Olsen, and K. Mosegaard (2005), Heat flux anomalies in Antarctica revealed by satellite magnetic data, *Science*, 309, 464–467.
- Morelli, A., and S. Danesi (2004), Seismological imaging of the Antarctic continental lithosphere: A review, *Global Planet. Change*, 42, 155–165, doi:10.1016/j.gloplacha.2003.12.005.
- O'Donnell, J. P., and A. A. Nyblade (2014), Antarctica's hypsometry and crustal thickness: Implications for the origin of anomalous topography in East Antarctica, *Earth Planet. Sci. Lett.*, 388, 143–155.
- Panter, K. S., P. R. Kyle, and J. L. Smellie (1997), Petrogenesis of a phonolite-trachyte succession at Mount Sidley, Marie Byrd Land, Antarctica, *J. Petrol.*, 38(9), 1225–1253.
- Paulson, T. S., and T. J. Wilson (2010), Evolution of Neogene volcanism and stress patterns in the glaciated West Antarctic Rift, Marie Byrd Land, Antarctica, *J. Geol. Soc. London*, 167, 401–416, doi:10.1144/0016-76492009-044.
- Pollard, D., R. M. DeConto, and A. A. Nyblade (2005), Sensitivity of Cenozoic Antarctic ice sheet variations to geothermal heat flux, *Global Planet. Change*, 49(1), 63–74.
- Pyle, M. L., D. A. Wiens, A. A. Nyblade, and S. Anandakrishnan (2010), Crustal structure of the Transantarctic Mountains near the Ross Sea from ambient seismic noise tomography, *J. Geophys. Res.*, 115, B11310, doi:10.1029/2009JB007081.
- Randall, D. E., and C. Mac Niocaill (2004), Cambrian palaeomagnetic data confirm a Natal Embayment location for the Ellsworth-Whitmore Mountains, Antarctica, in Gondwana reconstructions, *Geophys. J. Int.*, 157(1), 105–116.
- Reading, A. M. (2006), The seismic structure of Precambrian and early Palaeozoic terranes in the Lambert Glacier region, East Antarctica, *Earth Planet. Sci. Lett.*, 244, 44–57, doi:10.1016/j.epsl.2006.01.031.
- Reusch, A. M., A. A. Nyblade, M. H. Benoit, D. A. Wiens, S. Anandakrishnan, D. Voigt, and P. J. Shore (2008), Mantle transition zone thickness beneath Ross Island, the Transantarctic Mountains, and East Antarctica, *Geophys. Res. Lett.*, 35, L12301, doi:10.1029/2008GL033873.
- Ribe, N., A. Davaille, and U. R. Christensen (2007), Fluid dynamics of mantle plumes, in *Mantle Plumes*, pp. 1–48, Springer, Berlin.
- Ritzwoller, M. H., N. M. Shapiro, A. L. Levshin, and G. M. Leahy (2001), Crustal and upper mantle structure beneath Antarctica and surrounding oceans, *J. Geophys. Res.*, 106(12), 30,645–30,670.
- Roult, G., and D. Roulard (1992), Antarctica I: Deep structure investigations inferred from seismology: A review, *Phys. Earth Planet. Int.*, 84, 15–32.
- Sambridge, M., and K. Mosegaard (2002), Monte-Carlo methods in geophysical inverse problems, *Rev. Geophys.*, 40(3), 1009, doi:10.1029/2000RG000089.
- Schmandt, B., K. Dueker, G. Humphreys, and S. Hansen (2012), Hot mantle upwelling across the 660 beneath Yellowstone, *Earth Planet. Sci. Lett.*, 331–332, 224–236.
- Schopf, J. M. (1969), Ellsworth Mountains: Position in West Antarctica due to sea-floor spreading, *Science*, 164(3875), 63–66.
- Schroeder, D. M., D. D. Blankenship, D. A. Young, and E. Quartini (2014), Evidence for elevated and spatially variable geothermal flux beneath the West Antarctic Ice Sheet, *Proc. Natl. Acad. Sci. U.S.A.*, 111(25), 9070–9072.
- Schulte-Pelkum, V., and Y. Ben-Zion (2012), Apparent vertical Moho offsets under continental strike-slip faults from lithology contrasts in the seismogenic crust, *Bull. Seismol. Soc. Am.*, 102, 2757–1763.
- Shapiro, N. M., and M. H. Ritzwoller (2002), Monte-Carlo inversion for a global shear-velocity model of the crust and upper mantle, *Geophys. J. Int.*, 151, 88–105.
- Shapiro, N. M., and M. H. Ritzwoller (2004), Inferring surface heat flux distributions guided by a global seismic model: Particular application to Antarctica, *Earth Planet. Sci. Lett.*, 223, 213–224.
- Shen, W., M. H. Ritzwoller, V. Schulte-Pelkum, and F.-C. Lin (2012), Joint inversion of surface wave dispersion and receiver functions: A Bayesian Monte-Carlo approach, *Geophys. J. Int.*, 192(2), 807–836, doi:10.1093/gji/ggs050.
- Siddoway, C. S. (2008), Tectonics of the West Antarctic Rift System: New light on the history and dynamics of distributed intracontinental extension, in *Antarctica: A Keystone in a Changing World*, pp. 91–114, Natl. Acad. Press, Washington, D. C.
- Siddoway, C. S., S. L. Baldwin, P. G. Fitzgerald, C. M. Fanning, and B. P. Luyendyk (2004), Ross Sea mylonites and the timing of intracontinental extension within the West Antarctic rift system, *Geology*, 32(1), 57–60, doi:10.1130/G20005.1.
- Sieminski, A., E. Debye, and J.-J. Leveque (2003), Seismic evidence for deep low-velocity anomalies in the transition zone beneath West Antarctica, *Earth Planet. Sci. Lett.*, 216, 645–661, doi:10.1016/S0012-821X(03)00518-1.
- Stern, T. A., and U. S. ten Brink (1989), Flexural uplift of the Transantarctic Mountains, *J. Geophys. Res.*, 94(B8), 10,315–310,330.
- Studinger, M., R. E. Bell, W. R. Buck, G. D. Karner, and D. D. Blankenship (2004), Sub-ice geology inland of the Transantarctic Mountains in light of new aerogeophysical data, *Earth Planet. Sci. Lett.*, 220, 391–408, doi:10.1016/S0012-821X(04)00066-4.
- Stump, E., M. F. Sheridan, S. G. Borg, and J. F. Sutter (1980), Early Miocene subglacial basalts, the East Antarctic Ice Sheet, and uplift of the Transantarctic Mountains, *Science*, 207(4432), 757–759, doi:10.1126/science.207.4432.757.
- Sun, X., D. A. Wiens, A. Nyblade, S. Anandakrishnan, R. C. Aster, J. A. Chapat, A. D. Huerta, and T. J. Wilson (2013), Three dimensional crust and upper mantle velocity structure of Antarctica from seismic noise correlation, Abstract T12A-02 presented at 2013 Fall Meeting, AGU, San Francisco, Calif., 9–13 Dec.
- ten Brink, U. S., and T. A. Stern (1992), Rift flank uplifts and hinterland basins: Comparisons of the Transantarctic Mountains with the Great Escarpment of Southern Africa, *J. Geophys. Res.*, 97(B1), 569–585.
- ten Brink, U. S., S. Bannister, B. C. Beaudoin, and T. A. Stern (1993), Geophysical investigations of the tectonic boundary between East and West Antarctica, *Science*, 261, 45–50.
- van de Flierdt, T., S. R. Hemming, S. L. Goldstein, G. E. Gehrels, and S. E. Cox (2008), Evidence against a young volcanic origin of the Gamburtsev Subglacial Mountains, Antarctica, *Geophys. Res. Lett.*, 35, L21303, doi:10.1029/2008GL035564.
- van der Wal, W., P. L. Whitehouse, and E. J. Schrama (2015), Effect of GIA models with 3D composite mantle viscosity on GRACE mass balance estimates for Antarctica, *Earth Planet. Sci. Lett.*, 414, 134–143.
- Vogel, S. W., and S. Tulaczyk (2006), Ice-dynamical constraints on the existence and impact of subglacial volcanism on West Antarctic ice sheet stability, *Geophys. Res. Lett.*, 33, L23502, doi:10.1029/2006GL027345.
- Watson, T., A. Nyblade, D. A. Wiens, S. Anandakrishnan, M. Benoit, P. J. Shore, D. Voigt, and J. VanDecar (2006), P and S velocity structure of the upper mantle beneath the Transantarctic Mountains, East Antarctic craton, and Ross Sea from travel time tomography, *Geochem. Geophys. Geosyst.*, 7, Q07005, doi:10.1029/2005GC001238.
- Weaver, S. D., B. C. Storey, R. J. Pankhurst, S. B. Mukasa, V. J. DiVenere, and J. D. Bradshaw (1994), Antarctica-New Zealand rifting and Marie Byrd Land lithospheric magmatism linked to ridge subduction and mantle plume activity, *Geology*, 22, 811–814.
- Wessel, P., and W. H. F. Smith (1998), New, improved version of Generic Mapping Tools released, *Eos Trans. AGU*, 79(47), 579–579.
- Wilson, D. S., and B. P. Luyendyk (2006), Bedrock platforms within the Ross Embayment, West Antarctica: Hypotheses for ice sheet history, wave erosion, Cenozoic extension, and thermal subsidence, *Geochem. Geophys. Geosyst.*, 7, Q12011, doi:10.1029/2006GC001294.

- Wilson, D. S., and B. P. Luyendyk (2009), West Antarctic paleotopography estimated at the Eocene-Oligocene climate transition, *Geophys. Res. Lett.*, 36, L16302, doi:10.1029/2009GL039297.
- Wilson, T. J. (1995), Cenozoic trans-tension along the Transantarctic Mountains-West Antarctic Rift boundary, southern Victoria Land, Antarctica, *Tectonics*, 14(2), 531–545.
- Winberry, J. P., and S. Anandakrishnan (2004), Crustal structure of the West Antarctic rift system and Marie Byrd Land hotspot, *Geology*, 32(11), 977–980, doi:10.1130/G20768.1.
- Yang, Y., and D. W. Forsyth (2006), Regional tomographic inversion of the amplitude and phase of Rayleigh waves with 2-D sensitivity kernels, *Geophys. J. Int.*, 166, 1148–1160, doi:10.1111/j.1365-246X.2006.02972.x.
- Yang, Y., and M. H. Ritzwoller (2008), Teleseismic surface wave tomography in the western U.S. using the transportable array component of USArray, *Geophys. Res. Lett.*, 35, L04308, doi:10.1029/2007GL032278.
- Yang, Y., M. H. Ritzwoller, F.-C. Lin, M. P. Moschetti, and N. M. Shapiro (2008), Structure of the crust and uppermost mantle beneath the western United States revealed by ambient noise and earthquake tomography, *J. Geophys. Res.*, 113, B12310, doi:10.1029/2008JB005833.
- Zandt, G., H. Gilbert, T. J. Owens, M. Ducea, J. Saleeby, and C. H. Jones (2004), Active foundering of a continental arc root beneath the southern Sierra Nevada in California, *Nature*, 431, 41–46.
- Zhou, Y., F. A. Dahlen, and G. Nolet (2004), Three-dimensional sensitivity kernels for the surface-wave observables, *Geophys. J. Int.*, 158, 142–168, doi:10.1111/j.1365-246X.2004.02324.x.